

## Digital Control of Bonding Force for Gold Wire Bonding Machine

Xiaochu Wang\*, Zhongjun Zhu, Jian Gao, Xin Chen, and Yonggang Wu

School of Electromechanical Engineering, Guangdong University of Technology,  
Key Laboratory of Mechanical Equipment Manufacturing & Control Technology,  
Ministry of Education, Guangzhou, 510006, China

\*Corresponding author, e-mail: wangxc@gdut.edu.cn

### Abstract

*In order to digitally control the bonding force of a wire bonder precisely, this paper uses a DC solenoid as a force source, and by controlling the solenoid's current, which causes the electromagnetic force, we can control the bonding force that capillary applies. The bonding force control system in this paper is composed of PC (Personal Computer) and hypogyny MCU (Micro Controller Unit), which communicate using a RS485 interface. The digital value of a given bonding force is given by the PC to the MCU. By comparing the sampling current of the solenoid, and through PID regulation, D/A converter of the digital potentiometer and the solenoid driver circuit, the half-closed loop control system of bonding force is accomplished. Tuning of the PID parameters is accomplished with fuzzy adaptive control theory and simulated by Matlab simulink. The control system is tested by comparing the desired bonding force and the force actually applied and examining the relationship between bonding quality and bonding force.*

**Keywords:** Wire bonding, Digital control, Bonding force, Adaptive PID

**Copyright © 2013 Universitas Ahmad Dahlan. All rights reserved.**

### 1. Introduction

Wire bonding is by far the most popular interconnection technology because of its low cost and good performance. At present over 95% of the manufactured packages (in volume) are being wire bonded. Amongst various wire bonding processes, the ultrasonic wire bonding (UWB) has the advantages of fast bonding process, high productivity, excellent electrical performance, good heat conductivity and good corrosion resistance, so it has been widely used in various electronic packages [1-3]. The increasing demands for high speed signal propagation have led to significant advances in IC (Integrated Circuit) fabrication. With the ongoing demands for higher density and productivity of semiconductor packages, smaller pad sizes and finer pitches are required during the wire bonding process in the production lines. Therefore, improving the performance of a wire bonding machine is a big challenge [4-6].

The quality of the wire bonding is dependent on many subprocesses and material variables, such as the ultrasonic power, applied force, welding time, bond pad surface hardness, and interface temperature [6-7]. Therefore, these parameters should be set optimally to get the best bond quality. Before optimization, it is significantly important to get a fully understanding to the bonding mechanism and process. There are many descriptions of the bonding mechanism and process available [8-10]. E. Spaan et al [10]. modeled the wire bonding process from a numerical point of view to get a thorough understanding of the wire bonding process and optimize the parameters. Huang et al [6]. developed a methodology to optimize the bonding parameters, that is to use the explicit dynamic analysis results to reflect the real impact response under different CV (Constant Velocity) settings. SHU. et al [4]. used response surface methodology and regression analysis to optimize the bonding parameters. Ding et al [7]. analyzed the elasto-plastic large deformation taking place in ultrasonic wire bonding by means of 2-D and 3-D finite element method and focused on how important wire bonding parameters, such as bonding force and power affect the contact pressure along the wire-bonding pad interface, consequently the bond quality. For bond quality assessment, R. Rodwell et al [9]. introduce three ways: pull test, shear test and visual inspection.

Bonding force is one of the essential parameters of the wire bonding. The magnitude and the stability of the bonding force are significantly important for the bond quality. Fang et al

[11]. presented a methodology for a wire bonding force control system based on robust simultaneous optimal design of structure and control system, so that the overshoot of the bonding force and the effects of the fluctuation of the system parameters can be dealt with to fulfill the requirement of the advanced wire bonding system. Kim et al [3]. presented an impact force compensation algorithm designed for gold wire bonding processes, which uses a piezo forcesensor and contains a new algorithm design to reduce the impact force of the capillary when it contacts a silicon pad. To avoid bonding force drifting R. Pufall et al [12]. fixed a strain gauge to the bond arm to get a real-time recording of the bonding force. These works on bonding force control are very useful for a further research. However, there is very little work focus on designing a bonding force control system, and the control methodology to make sure the system output a stable bonding force, which is important for the control of the bonding process.

This paper focuses on the bonding force as it is one of the key parameters for bond quality. The purpose of this paper is to get an accurate and stable bonding force which is needed in wire bonding process to get a good bond quality. In order to achieve this purpose, the following works have been done. First a close loop bonding force control system uses solenoid current feedback is designed. Then, use incremental PID algorithm to control the system. For the tuning of the PID parameters, the fuzzy control theory is adopted, and the PID control system is simulated by Matlab simulink. Experiments are done to evaluate the performance of the system by comparing the desired bonding force and the force actually applied. In practical bonding process, the best bonding force is gained by examining the bonded joints. Through these experiments, we can see that this bonding force control system works well, and can provide an accurate and stable bonding force. This is important for the bonding quality control of a wire bonder.

## 2. Schematic of Bonding Force Given By the Capillary

The schematic of how the bonding force is applied to the capillary is shown in Figure 1. The capillary is installed in the front-end of the transducer, whilst the iron pad and the DC solenoid are at the rear-end. The solenoid produces a magnetic field that attracts the iron pad with a force  $F_1$ , the capillary applies a vertical downward force  $F_2$ , according to the lever principle,  $F_2 = (F_1 \times L_1) / L_2$ , therefore  $F_2$  is controllable by controlling  $F_1$ .

Due to the difference of the bonding parameters and different dimensions of gold wire, the bonding force should be adjustable with in the range of 0-180g. By calculation, the electromagnetic force should therefore be between 0-400g. This paper uses AX1625L solenoid, and its electromagnetic force curve is shown in Figure 2.13 This curve shows the data information of the solenoid's electromagnetic force while the gap between solenoid and iron pad is 0mm. The force is about 1500g at the 100% load rate and the power is 4W. For wire bonders, the gap is set at 1.5mm, so the force should be around 30% of which when the gap is 0mm ( i.e.  $\approx 450$ ). In order to get a 0-180g force, we can just adjust the current of the solenoid.

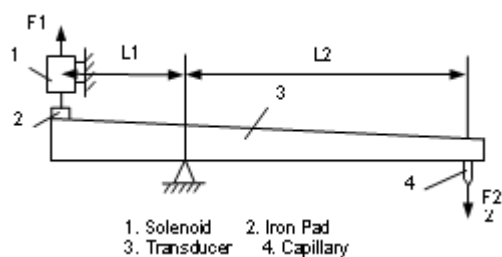


Figure 1. The schematic of how the bonding force is applied to the capillary

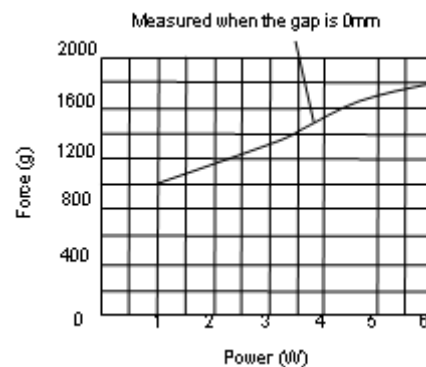


Figure 2. AX1625L solenoid's electromagnetic force curve

### 3. Bonding Force Control

Figure 3 shows the block diagram of bonding force control. The bonding force is proportional to the current of the solenoid. The PC sends a digital value of bonding force (0-255) whose resolution is 0.7g/bit to the MCU. Output from the MCU is then sent to the digital potentiometer as an input to regulate the output voltage which is amplified by an amplifier to drive the solenoid. The sampling current of the solenoid is converted to a digital value by the A/D converter, and then sent back to the MCU as a feedback. By adopting an incremental PID algorithm, the deviation between the given value and the real measured value is regulated to get an accurate and stable bonding force.

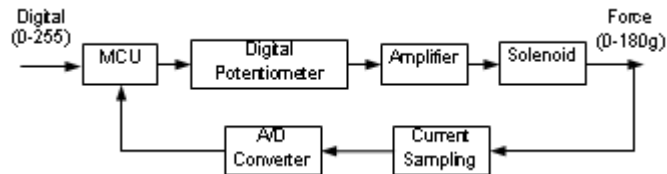


Figure 3. The block diagram of bonding force control

#### 3.1. Solenoid Driver and Current Control

The schematic of solenoid driver and current control is shown in Figure 4. In the process of the 1st bond, the PC sends the control signals F1C and F2C to enable analog switch A and disable analog switch B, so that the 1st bonding force control signal F1 gained from digital potentiometer is sent to drive the solenoid producing the solenoid current after being amplified. On the 2nd bond, analog switch A is off, and analog switch B is on. Output voltage from digital potentiometer F2C controls solenoid current of the 2nd bond. The current of the solenoid is then sampled by R5 and sent back to the MCU as a feedback after converted by the A/D converter to realize a closed loop control system of solenoid current.

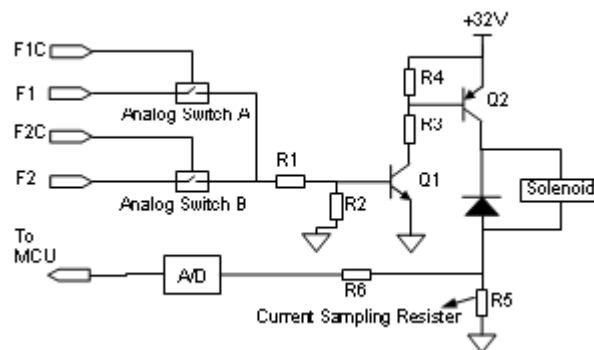


Figure 4. Schematic of solenoid driver and current control

#### 3.2. The Control Algorithm of Bonding Force

In the incremental PID algorithm, because PC output is a deviation, there should be less damage when a malfunction occurs, as there is no positive feedback in the algorithm, and  $u(k)$  is only related to the previous couple of samplings, a good result can be achieved just by weighting.

This paper adopts incremental PID algorithm.<sup>14</sup> The controller output is the deviation of every step of the process, which is represented as  $u(k)$ .

$$\Delta u(k) = u(k) - u(k-1)$$

$$\begin{aligned}
&= K_p e(k) + K_i \sum_{j=0}^{k-1} e(j) + K_d [e(k) - e(k-1)] - K_p \left\{ [e(k) - e(k-1)] + \frac{T}{T_i} \left( \sum_{i=0}^k e_i - \sum_{i=0}^{k-1} e_i \right) + \frac{T_d}{T} [e(k) - 2e(k-1)] \right\} \\
&= K_p [e(k) - e(k-1)] + K_i e(k) + K_d [e(k) - 2e(k-1) + e(k-2)] \\
&= K_p e(k) + K_i \sum_{j=0}^{k-1} e(j) + K_d [e(k) - e(k-1)] \tag{1}
\end{aligned}$$

where,  $T$  -- Sampling period

$T_i$  -- Integration time constant

$T_d$  -- Differential time constant

$K_p$  -- Proportional coefficient

$K_i$  -- Integration coefficient,  $K_i = K_p (T / T_i)$

$K_d$  -- Differential coefficient,  $K_d = K_p (T_d / T)$

$\Delta e(k)$  -- Deviation input for the  $K$ -th sampling,

$\Delta e(k) = e(k) - e(k-1)$ ,  $\square e(k-1) = e(k-1) - e(k-2)$

Equation (1) can also be written as:

$$\begin{aligned}
\Delta u(k) &= K_p [e(k) - e(k-1)] + K_p \frac{T}{T_i} e(k) + K_p \frac{T_d}{T} [e(k) - 2e(k-1) + e(k-2)] \\
&= Ae(k) - Be(k-1) + Ce(k-2) \tag{2}
\end{aligned}$$

where,  $A = K_p (1 + T / T_i + T_d / T)$

$B = K_p (1 + 2 T_d / T)$

$C = K_p (T_d / T)$

## 4. PID Parameters Tuning

### 4.1. The Mathematical Model of the Solenoid

A solenoid is an electrical device that produces an electromagnetic force when activated, turning electrical energy into mechanical energy.<sup>15</sup> This paper uses a DC solenoid, to the control of bonding force where the solenoid current is controlled with PID algorithm. In order to test PID algorithm's features and tune the PID parameters, the PID control system of the solenoid current is simulated.

Before simulation, the mathematical model must be established. The solenoid's structure and magnetic circuit are shown in Figure 5.

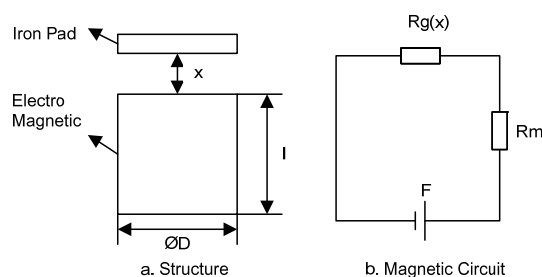


Figure 5. The structure and magnetic circuit of the solenoid

Magnetizer reluctance  $R_m$ :

$$R_m = \frac{l}{\mu \pi D^2 / 4} \tag{3}$$

Air gap reluctance  $R_g(x)$ :

$$R_g(x) = \frac{g-x}{\mu_0 \pi D^2 / 4} \tag{4}$$

The magnetomotive force of the exciting coil  $F$ :

$$F = Ni \quad (5)$$

Without consideration of magnetic saturation, the inductance of the solenoid  $L(x)$ :

$$L(x) = \frac{N^2}{R_m + R_g(x)} \quad (6)$$

Flux linkage equation:

$$\varphi = L(x) \times i \quad (7)$$

Motive voltage equation:

$$e = v i \frac{dL(x)}{dx} \quad (8)$$

Mechanical movement equation:

$$F_e - f = m \frac{dv}{dt} \quad (9)$$

$$f = \int_0^t v dt \quad (10)$$

Solenoid voltage equation:

$$u(t) = iR + \frac{d\varphi}{dt} + e \quad (11)$$

Electromagnetic force equation:

$$F_e = \frac{1}{2} i^2 \frac{dL(x)}{dx} \quad (12)$$

where,  $\mu$  -- The permeability of the magnetizer (H/cm)

$\mu_0$  -- The permeability of the air gas (H/cm)

$N$  -- The turns of the exciting coil

$I$  -- The current of the coil (A)

$v$  -- The velocity of the iron pad (cm/s)

$x$  -- The displacement of the iron pad (cm)

$m$  -- The mass of the iron pad (kg)

$R$  -- The resistance of the coil ( $\Omega$ )

$f$  -- The load (N)

#### 4.2. The Theory of Fuzzy Control

Fuzzy control is an intelligent control method based on fuzzy set theory, fuzzy linguistic variables, and fuzzy logic, which imitates the human fuzzy reasoning and decision-making processes. This method compiles the experience of the operators or experts into fuzzy rules during a training period. There after the signals are interpreted by the fuzzy rules and the output is sent to the actuator.

The block diagram of fuzzy control algorithm is shown in Figure 6. The key part is the fuzzy controller which is framed in the figure. The function of the fuzzy controller is realized by a computer program. The process of the fuzzy control is described as follows: the MCU gets the accurate control value by interrupted sampling, the error  $e$  is obtained by comparing the actual

and given value and is used as one of the inputs of the fuzzy controller. Then  $e$  is fuzzified and can be expressed in corresponding fuzzy language as a subset of the fuzzy linguistic set  $\tilde{e}$  ( $\tilde{e}$  is a fuzzy vector). According to the fuzzy control rules (fuzzy operator)  $\tilde{R}$  and the combination rules of the fuzzy reasoning, the fuzzy control value  $\tilde{u}$  is:

$$\tilde{u} = \tilde{e} \circ \tilde{R} \tag{13}$$

### 4.3. The Fuzzy Adaptive PID Controller Parameters Tuning and Its Simulation

The fuzzy adaptive PID control, by using the basic theory and method of fuzzy mathematic, turns the conditions and methods of the rules into fuzzy sets and stores them to the PC as knowledge bases. The PC then uses fuzzy reasoning and tunes the PID parameters to the optimum, according to the actual response of the system. The block diagram of the fuzzy adaptive PID control is shown in Figure 7.

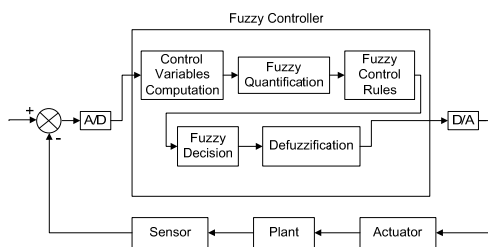


Figure 6. The block diagram of fuzzy control

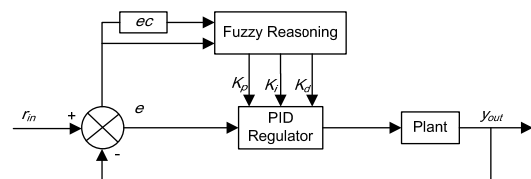


Figure 7. The block diagram of the fuzzy adaptive PID control

The fuzzy adaptive PID control is based on the PID algorithm, and by computing the present system error  $e$  and the error change rate  $ec$ , using the fuzzy rules and fuzzy reasoning, querying the fuzzy matrix tables, the PID parameters can be tuned. The key is to conclude the technical knowledge and the practical experience of the engineers to establish the appropriate fuzzy rules tables for  $K_p$ ,  $K_i$  and  $K_d$ .

Table 1-3 shows the fuzzy rules established for  $K_p$ ,  $K_i$  and  $K_d$

Table 1. The fuzzy rules table for  $K_p$

e	ec						
	NB	NM	NS	ZO	PS	PM	PB
NB	PB	PB	PM	PM	PS	ZO	ZO
NM	PB	PB	PM	PS	PS	ZO	NS
NS	PM	PM	PM	PS	ZO	NS	NS
ZO	PM	PM	PS	ZO	NS	NM	NM
PS	PS	PS	ZO	NS	NS	NM	NM
PM	PS	ZO	NS	NM	NM	NM	NB
PB	ZO	ZO	NM	NM	NM	NB	NB

Table 2. The fuzzy rules table for  $K_i$

e	ec						
	NB	NM	NS	ZO	PS	PM	PB
NB	PB	PB	PM	PM	PS	ZO	ZO
NM	PB	PB	PM	PS	PS	ZO	NS
NS	PM	PM	PM	PS	ZO	NS	NS
ZO	PM	PM	PS	ZO	NS	NM	NM
PS	PS	PS	ZO	NS	NS	NM	NM
PM	PS	ZO	NS	NM	NM	NM	NB
PB	ZO	ZO	NM	NM	NM	NB	NB

Table 3. The fuzzy rules table for  $K_d$

e	ec						
	NB	NM	NS	ZO	PS	PM	PB
NB	PB	PB	PM	PM	PS	ZO	ZO
NM	PB	PB	PM	PS	PS	ZO	NS
NS	PM	PM	PM	PS	ZO	NS	NS
ZO	PM	PM	PS	ZO	NS	NM	NM
PS	PS	PS	ZO	NS	NS	NM	NM
PM	PS	ZO	NS	NM	NM	NM	NB
PB	ZO	ZO	NM	NM	NM	NB	NB

Note for Table 1-3: NB-Negative Big, NM-Negative Medium, NS-Negative Small, ZO-Zero, PS-Positive Small, PM-Positive Medium, PB-Positive Big.

After establishing the fuzzy rules tables, define the range of e and ec as follow:

$$e, ec = \{-5, -4, -3, -2, -1, 0, 1, 2, 3, 4, 5\}$$

The subset of fuzzy set is:

$$e, ec = \{NB, NM, NS, ZO, PS, PN, PB\}$$

Assume the e, ec, Kp, Ki and Kd obey the normal distribution, the membership degree of each subset is obtainable. According to the copy table of each subset's membership degree and the fuzzy control model for each parameter, and by using the combined fuzzy reasoning, design the fuzzy rules tables for PID parameters. Query the tables for modified parameters and substitute them into the following equations to gain the three parameters.

$$\begin{aligned} K_p &= K'_p + \{e_i, ec_i\}_p \\ K_i &= K'_i + \{e_i, ec_i\}_i \\ K_d &= K'_d + \{e_i, ec_i\}_d \end{aligned} \tag{14}$$

In the process of online running, through processing the results of the fuzzy logic rules, querying the tables, and calculating, the control system tunes the PID parameters online. The process of the fuzzy adaptive PID control system's online self-tuning is shown in Figure 8.

Using incremental PID control algorithm and fuzzy control theory, the three parameters of PID controller can be tuned. A simulation program in Matlab is designed to simulate the solenoid current control system. The simulation results are shown in Figure 9 and Figure 10.

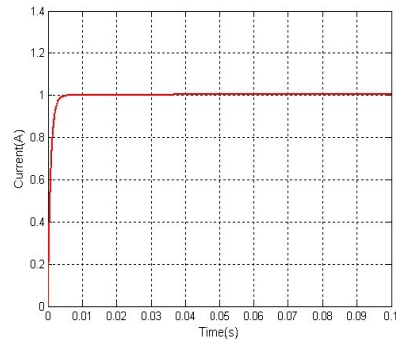
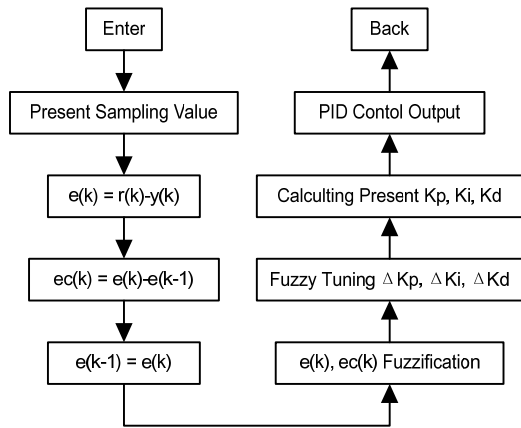


Figure 9. Input-Output response curve

Figure 8. The process of the fuzzy adaptive PID control system's online self-tuning

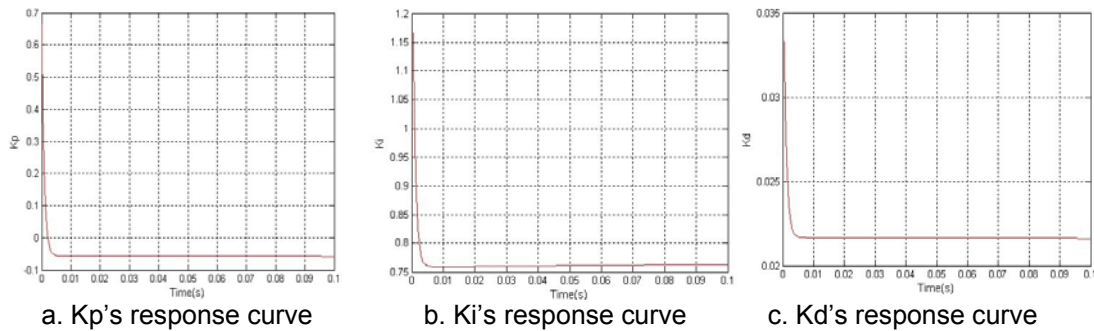


Figure 10. PID parameters response curve

### 5. Testing of Bonding Force

By changing the digital given value of the bonding force on the PC, the solenoid current will change accordingly, and consequently the electromagnetic force of the solenoid. Place a dynamometer under the capillary to measure the value of the bonding force. Data gained by dynamometer is shown in Table 4. For each digital given value, the bonding force applied to the capillary is measured 5 times by dynamometer to get the average force.

From the average force in Table 4, we can see that bonding force is basically stable with the exception of the upper and lower bounds. The relationship between digital given value and the average gained bonding force is shown in Figure 11. It shows that the relationship between digital given value and average gained bonding force is almost linear. The bonding force is proportional to the digital given value.

Table 4. Gained bonding force

Digital given value	Gained bonding force (g)					Average Force (g)
	1st	2nd	3rd	4th	5th	
10	19	21	21	22	19	20.4
20	25	24	25	23	24	24.2
30	32	30	31	29	32	30.8
40	36	37	35	34	34	35.2
50	42	42	41	40	41	41.2
60	45	46	45	47	47	46
70	49	51	50	50	52	50.4
80	60	61	58	59	60	59.6
100	75	80	76	77	78	77.2
120	110	110	115	110	113	111.6
140	135	136	140	138	133	136.4
160	145	150	155	153	151	150.8
180	180	175	178	180	175	177.6
200	220	221	226	223	219	221.8
220	255	253	254	256	255	254.6
240	267	270	260	270	265	266.4
255	280	290	275	310	300	291

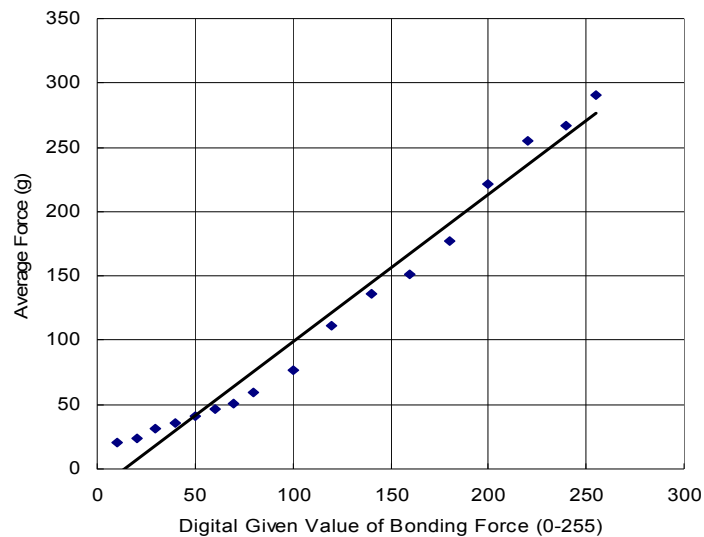


Figure 11. Relationship between digital given value and average gained bonding force

### 6. Bonding Quality Analysis

This control system was tested by gold wire bonding (diameters of the gold wire is 25.4μm) on to a copper frame. In order to get a good bonding quality, set the bonding parameters

as follows: duration spark: 10ms, current of spark: 200mA, 1st and 2nd bond's ultrasonic power: 70 (digital given value), time of 1st and 2nd bond: 10ms.

In the experiment, the parameters given above remained constant; the digital given value of the bonding force (0-255) is adjustable. The experiment consists of 100 bonds, including 100 bonded joints, 50 connections whose wire length is 2mm. Examples of the microscope pictures of different bonded joints are shown in Figure 12 and Figure 13. The pass and fail bonded joints statistics are shown in Table 5.

Table 5. Pass and fail bonded joints statistics

Digital given value (0-255)	Amount of bonded joints	Amount of pass joints		Amount of fail joints					Pass rate (%)
		#1	#2	#3	#4	#5	#6	#7	
0~20	100	10	72	3	0	6	1	8	82
25~45	100	25	73	0	0	0	0	2	98
50~70	100	24	75	0	0	0	0	1	99
75~95	100	20	68	1	4	0	0	7	88
100~120	100	8	59	2	21	0	5	5	67
125~145	100	2	49	8	30	0	5	6	51
150~170	100	1	27	8	50	0	7	7	28
175~195	100	0	9	8	70	0	10	3	9
200~220	100	0	0	0	98	0	0	2	0
225~245	100	0	0	0	98	0	0	2	0
250~255	100	0	0	0	99	0	0	1	0

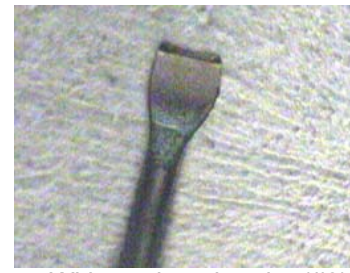
Figure 12 shows the pass bonded joints. Two bonded joints of one connection must be acceptable as following descriptions. The 1st bonded joint should be plump and smooth (#1), the 2nd bonded joint should be fish-tail shaped or without deep imprint (#2).



a. Plump and smooth (#1)



b. Fish-tail shape (#2)



c. Without deep imprint (#2)

Figure 12. Pass bonded joints

Figure 13 shows fail bonded joints. The following situations are failed. Wire-broken (#3), deep imprint (#4), loose joint (#5), ball squashed or unsmooth surface (#6), over sized joint or other situations (#7).

If the bonding force is too small or the frame surface is not clean enough, the bonded joint may be loose leading to the failure of the joints. However, when the bonding force is too large, it may cause damage to the gold wire and make deep imprint on the surface while bonding, or the wire could be broken while pulling the wire after the 1st bond. Incorrect settings of other parameters, such as tail too long, bonding time, power and time of ultrasonic energy may cause the bonded joints to be squashed or over sized joints may occurs.

We can see from Table 5, the best bonding force for the 1st and the 2nd bond is 25-70 (digital given value). In the bonding experiment, with different frames, parameter settings may need to be set differently.

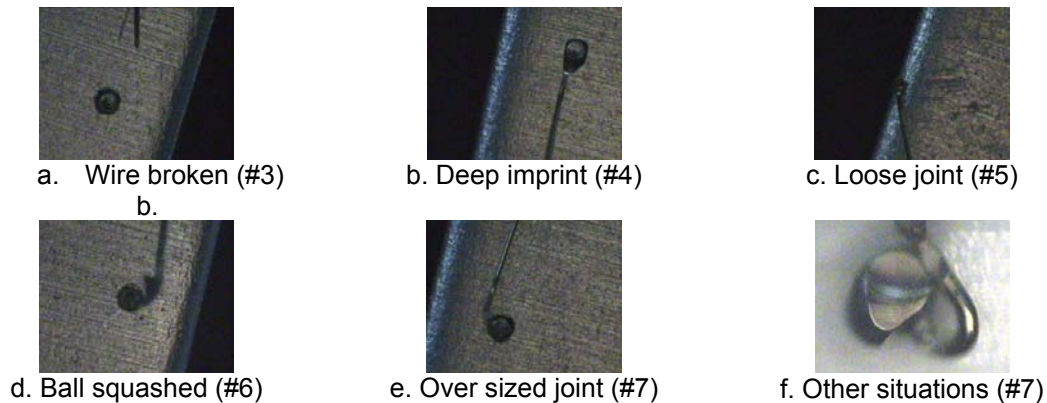


Figure 13. Fail bonded joints

## 7. Conclusion

The experimental study in this paper shows, by setting the proper gap between the solenoid and the iron pad, the solenoid can be used to control the bonding force. In the solenoid current control and driver system, the MCU receives digital given value of the bonding force from the PC, and also the sampling current of the solenoid from A/D converter, afterwards, outputs a precise and stable bonding force through the process of the incremental PID regulator and D/A converter of the digital potentiometer. The gained bonding force is proportional to the digital given value. The relationship between them is nearly linear.

For copper frame bonding, by setting the digital bonding force as 25-70 (digital given value), a better bonding effect can be achieved.

## Acknowledgments

This work is supported by National Basic Research Program of China (973 Program, Grant No. 2011CB013104), by Key Joint Project of National Natural Science Foundation of China (Grant No. U1134004), by the Specialized LED Sector Fund of Guangdong Provincial R&D Project (No.2011A081301001, 2012A080303004), and the Special Fund of High Education Disciplinary Construction Project from Guangdong Educational Department (No.2012CXZD0020).

## References

- [1] Harman GG, Albers J. The Ultrasonic Welding Mechanism as Applied to Aluminum and Gold Wire Bonding in Microelectronics. *IEEE Transactions on Parts, Hybrids, and Packaging*. 1977; 13: 406-412.
- [2] Tummala RR. *Editor*. Fundamental of Microsystems Packaging. New York: McGraw-Hill. 2001.
- [3] Jung-Han K, Chung-Hyuk Y. An Impact Force Compensation Algorithm Based on a Piezo Force Sensor for Wire Bonding Processes. *Control Engineering Practice*. 2008; 16: 685-696.
- [4] William K, SHU. Fine Pitch Gold Ball Bonding Optimization. *IEEE/CHMT European International Electronic Manufacturing Technology Symposium*. 1993: 37-41.
- [5] Rooney DT, Nager DP. and Shangguan D. Evaluation of Wire Bonding Performance, Process Conditions, and Metallurgical Integrity of Chip on Board Wire Bonds. *Microelectronics Reliability*. 1997; 45(2): 379-390.
- [6] Weidong H. *Computational Modeling and Optimization for Wire Bonding Process on Cu/Low-K Wafers*. 2009 International Conference on Electronic Packaging Technology and High Density Packaging. Beijing. 2009: 344-352.
- [7] Ding Y, Kim , JK, Tong P. Effects of Bonding Force on Contact Pressure and Frictional Energy in Wire Bonding. *Microelectronics Reliability*. 2006; 46 (7): 1101-1112.
- [8] Krzanowski JE. A transmission electron microscopy study of ultrasonic wire bonding Components. *IEEE Transactions on Hybrids, and Manufacturing Technology*. 1990; 13(1): 176-181.
- [9] Rodwell, D. A. Worrall. Quality Control in Ultrasonic Wire Bonding. *International Journal of Microcircuits and Electronic Packaging*. 1985;8(2):1-8.

- [10] Spaan E, Ooms E, van Driel, WD, Yuan CA, Yang DG, Zhang GQ. *Wire Bonding the Future: a Combined Experimental and Numerical Approach to Improve the Cu-Wirebonding Quality*. 2010 11th International Conference on Digital Object Identifier. Bordeaux, France. 2010: 1-4.
- [11] Fang L, Yuehong Y and Zhaoneng C. Robust simultaneous optimal design of structure and control for a wire bonding force control system. *Mechanical engineering Science*. 2007; 221(2): 177-186.
- [12] Information on <http://www.yaxin-china.com/ch/ProductView.asp?ID=189>
- [13] Pufall R. *Automatic Process Control of Wire Bonding*. Proceedings-Electronic Components and Technology Conference. Orlando, FL, USA. 1993:159-162.
- [14] Yonghua T. *Editor*. Novel PID Control and Its Application. Beijing: Mechanical Industry Press. 2002.
- [15] Tongjuan L, Nengqiang J. Simulation Analysis and Study on Transient Property of Electromagnet. *Low Voltage Apparatus*. 2005; 6: 14-17.
- [16] Yourui H, Ligu Q. *Editor*, PID Controller's Parameters Tuning and Realization. Beijing: Science Press. 2010.